OUKA
The University of Osaka
Institutional Knowledge Archive

| | |
|---|---|
| Title | Fundamental Studies of Electron Beam Welding of Heat-resistant Superalloys for Nuclear Plants (Report 5) : Mechanical Properties of Welded Joint |
| Author(s) | Arata, Yoshiaki; Terai, Kiyohide; Nagai, Hiroyoshi et al. |
| Citation | Transactions of JWRI. 1978, 7(2), p. 221-231 |
| Version Type | VoR |
| URL | https://doi.org/10.18910/6682 |
| rights | |
| Note | |

*The University of Osaka Institutional Knowledge Archive : OUKA*

https://ir.library.osaka-u.ac.jp/

The University of Osaka

# Fundamental Studies of Electron Beam Welding of Heat-resistant Superalloys for Nuclear Plants (Report 5)†

## – Mechanical Properties of Welded Joint –

Yoshiaki ARATA,* Kiyohide TERAI,** Hiroyoshi NAGAI,** Shigeki SHIMIZU,**
Toshiichi AOTA,** Keisuke SATOH** and Yoshikazu IKEMOTO.**

**Abstract**

*In this paper, the mechanical properties of base metal, its electron beam and TIG weld joint of superalloys for nuclear plants were made clear and compared with each other. As a result, it has been clarified that electron beam weld joint is superior to TIG weld joint and nearly comparable to base metal.*

### 1. Introduction

There are few reports on the mechanical properties especially at the elevated temperatures of electron beam weld joint of heat-resistant superalloys for nuclear plants, and these properties have not been fully studied yet.

In this report, the base metal, electron beam weld joint and TIG weld joint of above-mentioned superalloys were respectively investigated in the tensile properties, low-cycle fatigue properties at high temperatures, creep and creep rupture properties. Thereby, the mechanical properties of electron beam welded joint were made clear and proved to be superior to that of TIG weld joint.

### 2. Material used

**Table 1** shows the chemical composition and mechanical properties of such superalloys as Hastelloy-type, Inconel-type and Incoloy-type ones used. Three kinds of Hastelloy X of different heat are mentioned below as HAEN, HAEM and HVEN. **Table 2** shows the chemical composition of filler metal used for TIG welding.

### 3. Welding Procedure and Non-destructive Examination

Weld joints for various test specimens were made in such a way as shown below.

#### 3.1 Welding Conditions

Electron beam welding and TIG welding were respectively carried out in such conditions as shown in **Table 3** and **Table 4** after thinning the base metal off from 20mm to 15mm.

#### 3.2 Non-destructive Examination of Welds

All welds were examined by X-ray inspection. Thereby, it was proved that there was no weld defect in the welds.

### 4. Tensile Test Properties

#### 4.1 Testing Procedure

**Fig. 1** shows the configuration of tensile test specimen. The test specimen of weld joint was machined so that the weld metal zone was placed at the middle area of the gauge length. The central axis of test specimen complied with the rolling direction. "Shimazu Autograph" (capacity: 10 ton) was used as tensile testing machine. Tensile test was carried out at room temperature 600°C, 700°C, 800°C, 900°C and 1000°C in accordance with both "Method of Tensile Test for Metallic Materials" (JIS Z 2241) and "Method of High Temperature Tensile Test for Iron and Steel" (JIS G 0567). Strain rate was kept constant at 0.3%/min up to 0.2% proof stress and thereafter at 7.5%/min.

#### 4.2 Results and Discussion

**Fig. 2** shows an example of test results of base metal, electron beam weld joint and TIG weld joint at room temperature and elevated temperetures.

There is no appreciable difference among base metal and weld joints in tensile strength. As far as it concerns with 0.2% proof stress, TIG weld joint is superior to

† Received on October 22nd, 1978
* Professor and Director
** Kawasaki Heavy Industries, Ltd.

**Table 1** Chemical Composition and Mechanical Properties of Base Metal used

| Material | Mark | Thickness (mm) | * Melting Process | Final Heat Treatment | Grain Size (ASTM) | Mechanical Properties 0.2% P.S (kg/mm²) | T.S (kg/mm²) | El. (%) | RA (%) | Chemical Composition (%) C | Si | Mn | P | S | Ni | Cr | Co | Mo | W | Nb+Ta | Al | Ti | B | Fe | Gaseous Contents (ppm) O | N Sol. | N Insol. | N Total. |
|---|---|---|---|---|---|---|---|---|---|---|---|---|---|---|---|---|---|---|---|---|---|---|---|---|---|---|---|---|
| Hastelloy X | HAEN | 20 | AE | 1120°Cx18Min W.Q. | 1~4 | 30.4 | 71.1 | 59.0 | 65.0 | 0.066 | 0.48 | 0.88 | 0.016 | <0.002 | Bal. | 21.36 | 1.77 | 9.05 | 0.45 | — | 0.07 | 0.15 | 0.002 | 19.09 | 30 | 405 | 42 | 447 |
| | HAEM | | | 1150°Cx50Min W.Q. | 5~6 | 38.7 | 75.0 | 47.6 | — | 0.068 | 0.37 | 0.59 | 0.012 | <0.002 | | 20.74 | 1.03 | 8.70 | 0.50 | — | 0.21 | 0.02 | 0.001 | 18.23 | 20 | 248 | 20 | 268 |
| | HVEN | | VE | 1120°Cx18Min W.Q. | 1-6 | 34.3 | 73.8 | 49.3 | 56.9 | 0.084 | 0.17 | 0.84 | 0.001 | <0.002 | | 20.70 | 1.59 | 9.20 | 0.55 | | 0.22 | 0.19 | 0.002 | 18.53 | 50 | 306 | 16 | 322 |
| Inconel 625 | Inl 625AE | | AE | 1000°Cx1Hr W.Q. | 6 | 45.5 | 90.1 | 46.8 | — | 0.053 | 0.28 | 0.24 | 0.003 | <0.002 | | 22.09 | 0.06 | 8.81 | 0.69 | 3.53 | 0.24 | 0.13 | — | 2.54 | 30 | 44 | 211 | 255 |
| Inconel 617 | Inl 617V | | V | 1177°Cx1Hr W.Q. | 3~4 | 30.0 | 74.6 | 70.0 | 57.0 | 0.066 | 0.17 | 0.02 | 0.004 | <0.002 | | 21.24 | 12.60 | 9.00 | — | — | 0.93 | 0.52 | — | 1.45 | 40 | 244 | 180 | 424 |
| Incoloy 800 | Iny 800V | | V | 1100°Cx1.5 Hr W.Q. | 2.5 | 22.1 | 58.2 | 52.0 | 72.1 | 0.056 | 0.37 | 0.77 | 0.010 | 0.002 | 32.13 | 21.21 | 0.50 | 0.18 | — | — | 0.51 | 0.59 | — | Bal. | 60 | 32 | 93 | 125 |
| Incoloy 807 | Iny 807A | | A | 1230°Cx3Hr W.Q | 1 | 25.7 | 64.1 | 52.2 | 60.3 | 0.057 | 0.50 | 0.70 | 0.002 | 0.002 | 40.10 | 20.58 | 8.28 | 0.20 | 4.85 | 0.99 | 0.47 | 0.24 | — | | 70 | 68 | 144 | 212 |

* AE : Air Melting followed by Electroslag Remelting
VE : Vacuum Induction Melting followed by Eelctroslag Remelting.
V : Vacuum Induction Melting.
A : Air Melting.

**Table 2** Chemical Composition of Filler Metal for TIG Welding used

| Material | Chemical Composition (%) C | Si | Mn | P | S | Ni | Cr | Co | Mo | W | Nb+Ta | Al | Ti | B | Fe | Cu |
|---|---|---|---|---|---|---|---|---|---|---|---|---|---|---|---|---|
| Hastelloy X | 0.07 | 0.42 | 0.35 | 0.013 | <0.005 | Bal. | 21.56 | 1.00 | 8.97 | 0.51 | — | — | — | 0.002 | 17.80 | — |
| Inconel 625 | 0.015 | 0.32 | 0.32 | 0.004 | <0.005 | | 21.53 | Tr. | 8.86 | — | 3.74 | 0.16 | 0.14 | — | 2.62 | — |
| Inconel 617 | 0.08 | 0.16 | 0.03 | — | <0.007 | | 22.27 | 12.45 | 9.13 | — | — | 0.89 | — | — | 0.50 | — |
| Inconel 82 | 0.01 | 0.17 | 2.92 | — | 0.007 | | 19.77 | — | — | — | 2.59 | — | 0.35 | — | 0.38 | 0.03 |
| Incoloy 800 | 0.09 | 0.14 | 3.55 | 0.002 | 0.007 | 34.17 | 20.25 | — | — | — | — | 0.24 | 0.27 | — | Bal. | — |
| Incoloy 807 | 0.06 | 0.38 | 0.75 | 0.002 | 0.009 | 39.16 | 20.62 | 7.93 | — | 4.89 | — | 0.39 | 0.46 | — | | — |

Notes; Melting Process : Vacuum Induction Melting

**Table 3** Electron Beam Welding Conditions

| Joint Configuration | Welding Conditions Pch (Torr) | $D_F$ (mm) | $a_b$ (mm) | $I_b$ (mA) | $V_b$ (kV) | $v_b$ (cm/min) |
|---|---|---|---|---|---|---|
| 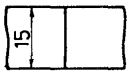  | $5\times10^{-4}$ | 225 | 1.04 | 40 | 150 | 60 |

**Table 4** TIG Welding Conditions

| Joint Configuration | Built-up Sequence | Welding Conditions Pass | Dia. of Filler Metal (mm) | Welding Current (A) | Arc Voltage (V) | Welding Speed (mm/min) | Shield Gas Flow (l/min) Torch | Back-up |
|---|---|---|---|---|---|---|---|---|
|   | 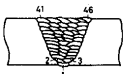  | 1 ~ 3 | 1.2 | 60 ~ 70 | 9 ~ 10 | 50 ~ 60 | 6 | 10 |
| | | 4 ~ 46 | 1.2 | 70 ~ 80 | 10 ~ 11 | | | – |

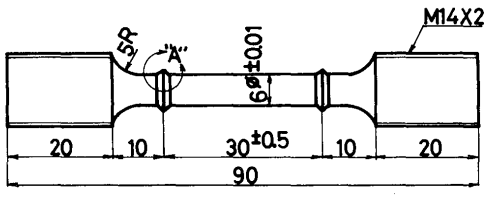


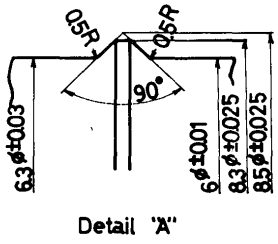


**Fig. 1** Configuration of Tensile Test Specimen

electron beam weld joint irrespective of temperature, and base metal has the lowest value.

In the elongation and reduction of area, electron beam weld joint falls far below the base metal but is superior to TIG weld joint. In any case, the ductility becomes poorest around 700°C approximately. **Table 5** shows the ratio of elongation and reduction of area for weld joint at 800°C, 900°C and 1000°C as compared with base metal. It is clear from this table that elentron beam weld joint has higher ductility than TIG weld joint.

## 5. Low-cycle Fatigue Properties at Elevated Temperatures

### 5.1 Testing Procedure

#### 5.1.1 Test Specimen

**Fig. 3** shows the configuration of fatigue test specimen. In case of weld joint, the weld metal zone was placed at the middle area of gauge length. The central axis of test apecimen complied with the rolling direction.

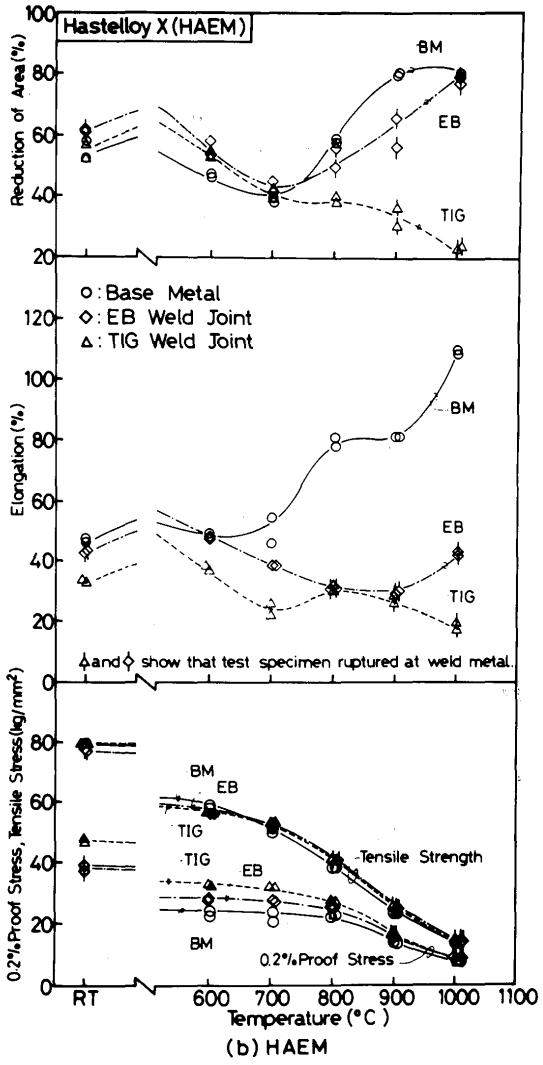


Fig. 2 Tensile Properties of Base Metal and Weld Joint at Room and Elevated Temperature for Hastelloy X (HAEM)

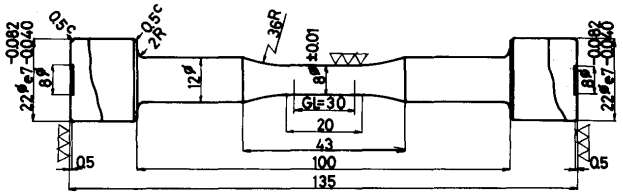


Fig. 3 Configuration of Fatigue Test Specimen

Table 5 Comparison of Ductility between Electron Beam and TIG Weld Joint

| Material | Mark | Welding Process | 800°C | | 900°C | | 1000°C | |
|---|---|---|---|---|---|---|---|---|
| | | | A | B | A | B | A | B |
| Hastelloy X | HAEN | EB | 0.79 | 0.96 | 0.42 | 0.85 | 0.40 | 0.89 |
| | | TIG | 0.33 | 0.31 | 0.21 | 0.31 | 0.20 | 0.40 |
| | HAEM | EB | 0.39 | 0.91 | 0.36 | 0.75 | 0.72 | 0.96 |
| | | TIG | 0.39 | 0.67 | 0.33 | 0.42 | 0.31 | 0.29 |
| | HVEN | EB | 1.23 | 1.37 | 0.98 | 1.22 | 0.84 | 1.41 |
| | | TIG | 0.42 | 0.75 | 0.49 | 1.04 | 0.50 | 1.51 |
| Inconel 625 | Inl 625AE | EB | 0.87 | 1.00 | 0.79 | 0.80 | 0.68 | 0.98 |
| | | TIG | 0.61 | 0.97 | 0.55 | 0.98 | 0.45 | 0.99 |
| Inconel 617 | Inl 617V | EB | 0.66 | 1.19 | 0.40 | 0.87 | 0.47 | 1.06 |
| | | TIG | 0.55 | 0.92 | 0.35 | 0.84 | 0.48 | 1.11 |
| Incoloy 800 | Iny 800V | EB | 0.81 | 0.90 | 0.72 | 0.87 | 0.54 | 0.96 |
| | | TIG | 0.36 | 0.53 | 0.37 | 0.88 | 0.34 | 0.90 |
| Incoloy 807 | Iny 807A | EB | 1.00 | 2.37 | 0.68 | 1.39 | 0.99 | 2.08 |
| | | TIG | 1.27 | 1.88 | 0.80 | 1.22 | 0.90 | 2.00 |

Notes; A : Elongation's Ratio, Weld Joint to Base Metal
B : Ratio of Reduction of Area, Weld Joint to Base Metal

### 5.1.2 Testing Machine

Testing machine consists of electro-hydraulic loading system (±10 ton) and heating system by P.I.D controlled induction heating. The strain of the specimen is detected by DTF-type extensometer, and controlled axially. Meanwhile, the temperature is also detected by the PR13% thermocouple which is attached to the middle area of the specimen by resistance welding. The temperature is controlled at the test temperature within ±2°C. The temperature of specimen is always highest at the middle area of the specimen. However, temperature difference in the gauge length is satisfactorily within 10°C.

### 5.1.3 Test Conditions

Low cycle fatigue test was carried out at the strain rate of 0.1% $sec^{-1}$ under the axially controlled strain of triangular wave form. The test was also conducted at the temperature of both 900°C and 1000°C.

### 5.2 Test Results and Discussion

Fig. 4 shows the schematic explanation of strain rate $\dot{\varepsilon}$, total strain range $\varepsilon_{tR}$ and plastic strain range $\varepsilon_{pR}$ which are below mentioned.

Figs. 5 to 7 shows typical examples at 900°C which are arranged in both $\varepsilon_{tR}$ $-N_{50}$ diagram and $\varepsilon_{pR}$ $-N_{50}$ diagram. $N_{50}$ is herein defined as number of cycle to failure at which tensile load decreases to the half value of initial one.

In general, nonlinear relation and linear one can be recognized in $\varepsilon_{tR}$ $-N_{50}$ diagram and $\varepsilon_{pR}$ $-N_{50}$ one respectively. Therefore, long-time fatigue life can be extrapolated from this linear relation between $\varepsilon_{pR}$ and $N_{50}$. From these figures, the fatigue life of electron beam weld joint is superior to that of TIG weld joint and equal to

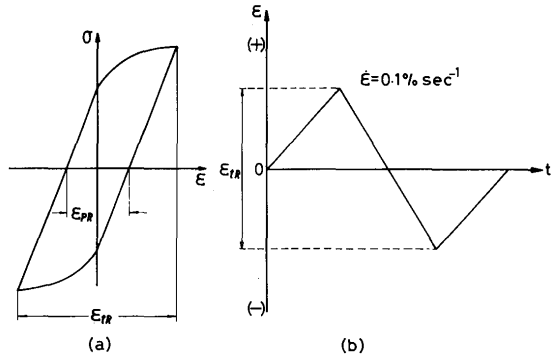


Fig. 4 Schematic Explanation of $\varepsilon_{tR}$, $\varepsilon_{pR}$ and Strain Pattern

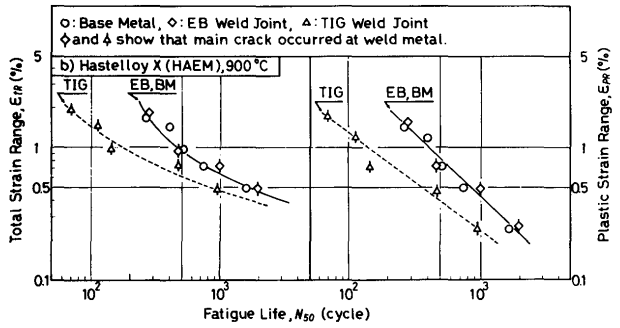


Fig. 5 Fatigue Properties of Base Metal and Weld Joint at 900°C for HAEM

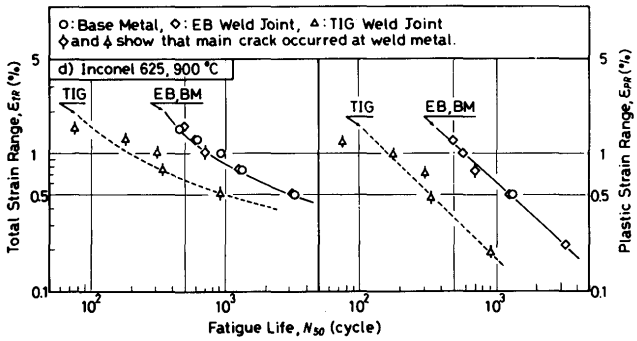


Fig. 6 Fatigue Properties of Base Metal and Weld Joint at 900°C for Inconel 625

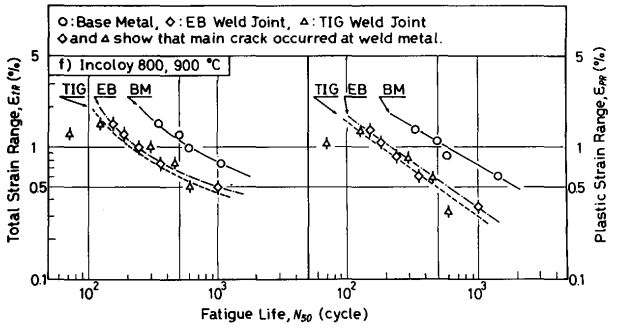


Fig. 7 Fatigue Properties of Base Metal and Weld Joint at 900°C for Incoloy 800

that of base metal in most cases. Test results at 1000°C showed similar tendency.

Concerning the fracture position, all the TIG weld joints fractured at the weld metal. On the other hand, electron beam weld joint fractured at base metal in some cases and at weld metal zone in other ones. The fracture at the weld metal generally results in the fatigue strength reduction.

**Table 6** shows the $N_{50}$ at $\varepsilon_{tR}$ of 0.5% for base metal and weld joints at 900°C and 1000°C respectively and the ratio of this fatigue life for weld joint as compared with base metal. The value in the parentheses shows the results at 1000°C.

At 900°C, electron beam weld joint of HAEM, HVEN, Inconel 625 and Incoloy 807 has the equal fatigue strength to the base metal. However, electron beam weld joint of HAEN, Inconel 617 and Incoloy 800 and all the TIG weld joints are inferior to the half of the base metal approximately. Meanwhile, electron beam weld joint of Inconel 625 and Incoloy 807 is equal to the base metal at 1000°C. The ratio of fatigue strength for electron beam weld joint of HAEN, HVEN and Inconel 617 is 0.6 approximately, and that of TIG weld joint is less than 0.5 approximately.

As mentioned above, the electron beam weld joint is clearly superior to TIG weld joint. It was mentioned in 4.2 that the ductility of the base metal was superior to that of the weld joint in tensile test and that electron beam weld joint showed higher ductility than TIG weld joint. It is generally recognized that the low-cycle fatigue strength under the constant repeated strain at elevated temperatures is largely dependent upon the ductility in tensile test.[1] The results obtained in the fatigue test nearly agree with the ductility in tensile test.

## 6. Creep and Creep Rupture Properties

### 6.1 Testing Procedure

#### 6.1.1 Test Specimen

**Figs. 8 and 9** show the configuration of creep and creep rupture test specimen respectively. In case of weld joint, the weld metal zone was placed at the middle area of gauge length. The central axis of test specimen complied with the rolling direction.

#### 6.1.2 Testing Machine

Creep testing machine used is lever-type and single type one in which elongation between two ridges can be measured. Creep rupture testing machine used is lever-type and multiple type one which has six strings to be able to test three specimens in one string at the same time. In both testing machines, loading capacity, lever ratio and test temperature are 1 ton, 10:1 and Max.

Table 6 Comparison of Fatigue Life between Electron Beam and TIG Weld Joint at 900°C (1000°C)

| Material | Mark | $N_{50}$($\varepsilon_{tr}$=0.5%) | | | $N_{50.\,WJ}/N_{50.\,BM}$ | |
|---|---|---|---|---|---|---|
| | | BM | EB | TIG | EB | TIG |
| Hastelloy x | HAEN | 1400 | 680 | 390 | 0.49 | 0.28 |
| | | (1500) | ( 900) | (440) | (0.60) | (0.29) |
| | HAEM | 1700 | 1700 | 800 | 1 | 0.47 |
| | HVEN | 1300 | 1300 | 620 | 1 | 0.48 |
| | | (1450) | (1000) | (580) | (0.69) | (0.40) |
| Inconel625 | Inl 625AE | 3300 | 3300 | 1000 | 1 | 0.30 |
| | | (3300) | (3300) | (420) | ( 1 ) | (0.13) |
| Inconel 617 | Inl 617V | 1000 | 670 | 880 | 0.67 | 0.88 |
| | | (1050) | ( 660) | (660) | (0.63) | (0.63) |
| Incoloy 800 | Iny 800V | 5000 | 1000 | 680 | 0.20 | 0.14 |
| Incoloy 807 | Iny 807A | 1250 | 1250 | 350 | 1 | 0.28 |
| | | (1200) | (1200) | (550) | ( 1 ) | (0.46) |

Notes; $N_{50}$: Fatigue Life defined as Number of Cycles at which Load decreases to half of Initial one
$N_{50.\,WJ}$ : Fatigue Life $N_{50}$ of Weld Joint
$N_{50.\,BM}$ : Fatigue Life $N_{50}$ of Base Metal
BM : Base Metal
EB : Electron Beam Weld Joint
TIG : TIG Weld Joint

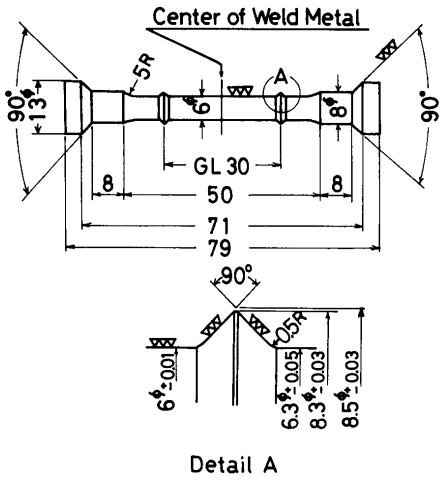


Fig. 8 Configuration of Greep Test Specimen

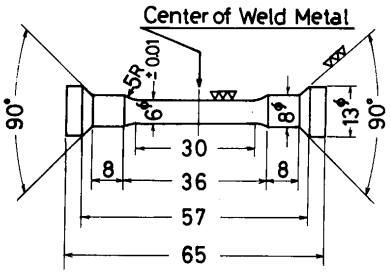


Fig. 9 Configuration of Creep Rupture Test Specimen

1100°C respectively. The accuracy of temperature and load satisfies the requirements specified in "Method of Tensile Creep Test for Metallic Materials" (JIS Z 2271).

### 6.1.3 Testing Method

Creep test was carried out for base metal, electron beam weld joint and TIG weld joint of HAEN, HAEM, HVEN, Inconel 625, Inconel 617, Incoloy 800 and Incoloy 807. Creep rupture test was also carried out for the weld joint of these superalloys. These tests were conducted at 900°C in the air under the constant load in accordance with "Method of Tensile Creep Test for Metallic Materials" (JIS Z 2271) and "Method of Creep Rupture Test for Metallic Materials" (JIS Z 2272).

In the creep test, temperature was automatically recorded and measured at the middle area and both edges in the gauge length (GL=30mm). In the creep rupture test, temperature was also recorded and measured at the middle area of gauge length (GL=30mm). In these tests, temperature was controlled at 900°C within the temperature range of ±3°C.

The elongation between two ridges was measured twice a day at both left and right side of test specimen in the creep test. The creep strain was defined as the mean value of the elongations measured at both sides of test specimen.

### 6.2 Test Results and Discussion

#### 6.2.1 Creep Properties

**(1) Creep Curve**

**Fig. 10** shows the creep curves of base metal, electron beam weld joint and TIG weld joint for HAEM. The weld joint is obviously superior to the base metal in the creep resistance, and TIG weld joint shows more creep resistance than electron beam weld joint.

In the creep curve obtained herein, primary, secondary and tertiary creep stage is not clear. Therefore, it is very difficult to decide the time to start secondary and tertiary creep.

**(2) Creep Strain Rate**

As mentioned above, every creep stage was not obvious in this experiment. The results were arranged in secondary creep rate vs time diagram to make creep behavior clear. Creep strain rate was herein calculated by the following formula.

$$\dot{\varepsilon}_n = \frac{\varepsilon_n - \varepsilon_{n-1}}{t_n - t_{n-1}}$$

where $\dot{\varepsilon}_n$ : secondary creep rate at the time of $t_n$
$\varepsilon_n$ : total strain measured at the time of $t_n$
$\varepsilon_{n-1}$ : total strain measured at the time of $t_{n-1}$

**Fig. 11** shows the relation between secondary creep rate and time for base metal, electron beam weld joint and TIG weld joint of HAEM. It is easy to define the creep behavior from this figure. Primary creep stage can be defined as the range where creep strain rate decreases with the elapse of time. Secondary creep stage can be also defined as the region of constant strain rate. Tertiary creep stage corresponds to the region where creep strain rate increases drastically with the elapse of time.

**(3) Secondary Creep Rate**

**Fig. 12** shows the relation between secondary creep rate and initial applied stress for base metal, electron beam weld joint and TIG weld joint of HAEM. In this figure, the linear relation is recognized easily. It may be safely said in this experiment that secondary creep rate of base metal is larger than that of weld joint at arbitrary initial applied stress but that electron beam weld joint is nearly comparable to the base metal.

#### 6.2.2 Creep Rupture Properties

**(1) Rupture Strength**

**Fig. 13** shows the relation between initial applied stress and time to rupture for base metal, electron beam weld joint and TIG weld joint of every superalloy.

There is no appreciable difference of creep rupture strength between base metal and weld joint for HAEN and HAEM. For HVEN, electron beam weld joint is nearly equal to base metal in creep rupture strength. However,

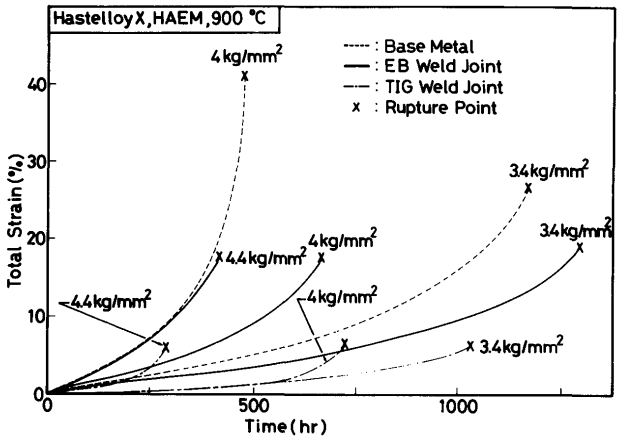


Fig. 10 Creep Curves for Base Metal and Weld Joint of Hastelloy X (HAEM)

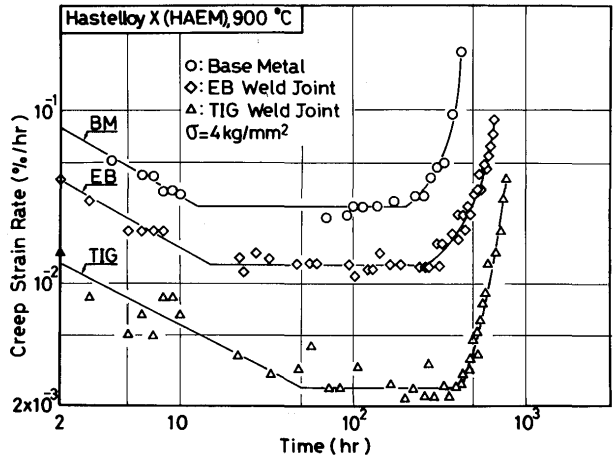


Fig. 11 Creep Strain Rate Curves for Base Metal and Weld Joint of Hastelloy X (HAEM)

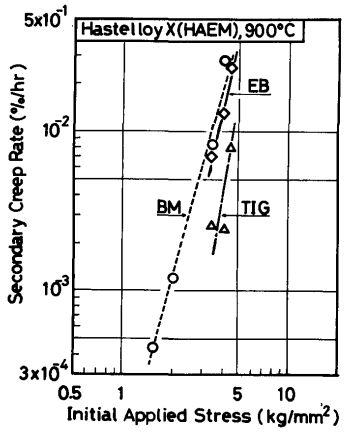


Fig. 12 Initial Applied Stress vs Secondary Creep Rate for Hastelloy X (HAEM)

TIG weld joint is far inferior to base metal. This reduction of creep rupture strength becomes more remarkable

in the long time to rupture. In this case, fracture takes place at the base metal. The reason of this reduction is not clear.

There is also no appreciable difference of creep rupture strength between base metal and weld joint for Inconel 625, Inconel 617 and Incoloy 807. In case of Incoloy 800, however, electron beam weld joint is nearly equal to base metal, and TIG weld joint is clearly inferior to base metal. In this case, fracture takes place at base metal for electron beam weld joint and at weld metal zone for TIG weld joint.

### (2) Fracture Ductility

**Fig. 14** shows the relation between elongation and time to rupture for base metal, electron beam weld joint and TIG weld joint of every superalloy. In any case, the elongation is clearly apt to decrease with the elapse of time to rupture. In the elongation and reduction of area, base metal is superior to weld joint. Electron beam weld joint, however, is superior to TIG weld joint and nearly comparable to base metal.

The elongation and reduction of area for the specimen in which fracture takes place at the weld metal zone is less than that for the specimen in which it takes place at the base metal.

### 6.2.3 Evaluation of Creep and Creep Rupture Properties

In case of the fracture of welded pipe with circumferential joint due to the internal pressure, peculiar deformation is considered to take place in case that there is the difference of secondary creep rate between base metal and weld metal. Thereby, shear force and bending moment acts at the weld metal and heat affected zone as schematically shown in **Fig. 15**. As a result, hoop stress acts due to the shear force, and tensile and compressive stress also acts axially due to the bending moment. These augmented stresses are superposed to the usual stress condition under the internal pressure. Therefore, the fracture takes place at the welds under high local stress. In this point of view, it is desirable that there is no difference of secondary creep rate between base metal and weld metal.

Internal pressure creep rupture test was carried out at the temperature of 900°C and under the internal pressure of 45.5 kg/cm$^2$G and 34.5 kg/cm$^2$G for the pipe of HAEM base metal, its electron beam and TIG weld joint which was 62mm and 3mm in outside diameter and wall thickness respectively. **Table 7** shows the test results under the internal pressure of 45.5 kg/cm$^2$G. It is clear from the appearance after fracture that the deformation of electron beam weld metal is nearly as large as the base metal and that peculiar deformation due to the difference

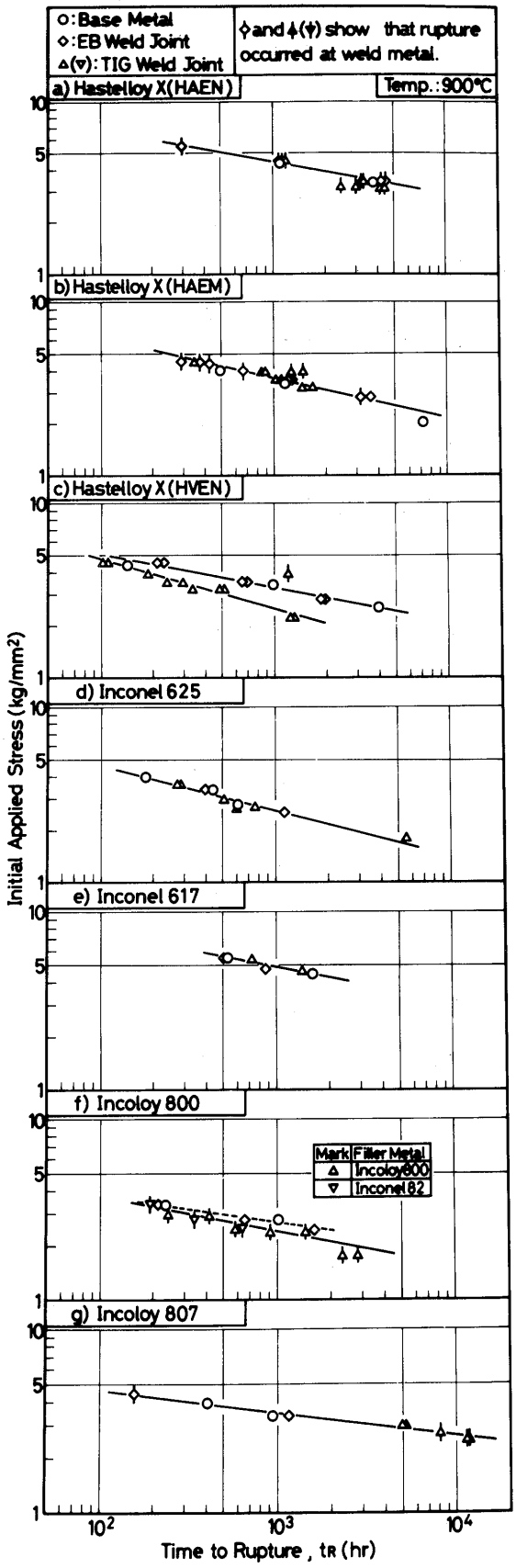


Fig. 13 Initial Applied Stress vs Time to Rupture for Base Metal and Weld Joint

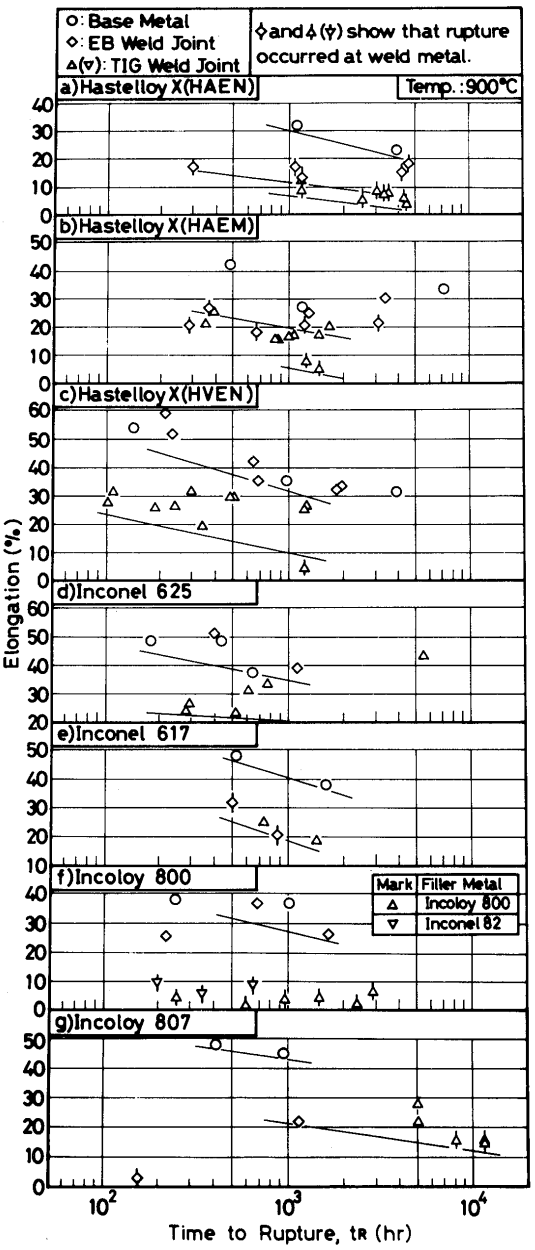


Fig. 14 Relation between Time to Rupture and Elongation for Base Metal and Weld Joint

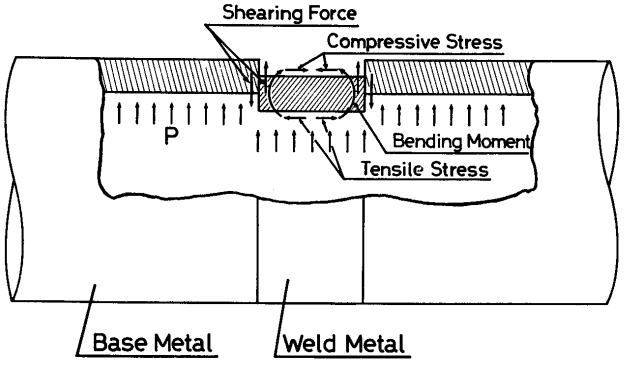


Fig. 15 Schematic Explanation of Creep Deformation of Welded Pipe with Circumferencial Weld Joint under Internal Pressure

Table 7 Comparison of Internal Pressure Creep Rupture Test Results

| Kind of Specimen | Temperature (°C) | Internal Pressure (kg/cm²G) | Time to Rupture (h) | Specimen's Appearance after Fracture |
|---|---|---|---|---|
| Base Metal | 900 | 45.5 | 271.3 | 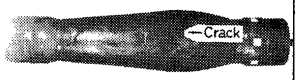 |
| EB Welded Joint | | | 173.5 | 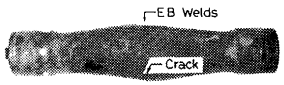 |
| TIG Welded Joint | | | 82.4 | 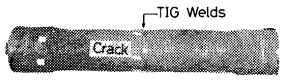 |



of secondary creep rate is not observed herein. Furthermore, the time to rupture of this weld joint is rather close to that of base metal than TIG weld joint mentioned below. Meanwhile, the peculiar deformation resulting from the difference of secondary creep rate is observed in case of TIG weld joint. The time to rupture of this weld joint is far less than that of the base metal due to the high local stress augmented in the welds. The test results under the internal pressure of 34.5 kg/cm$^2$G showed the same tendency. As shown above in Fig. 12, the secondary creep rate of its TIG weld joint is far smaller than that of HAEM base metal in uniaxial creep test. However, the secondary creep rate of its electron beam weld joint is nearly comparable to that of base metal. Therefore, internal pressure creep properties of the welded pipe with circumferential joint can be evaluated easily from the uniaxial creep properties of weld joint. It is most desirable that the secondary creep rate of weld joint is equal to that of base metal in uniaxial creep test.

As the correlation between secondary creep rate and elongation is recognized in **Fig. 16**,[2] secondary creep rate can be given from the elongation. Therefore, if weld joint is equivalent to base metal in the elongation, secondary creep rate of weld joint is considered to be nearly equal to that of base metal. Furthermore, creep rupture strength must be taken into consideration as one of important criteria to evaluate the weld joint.

**Table 8** shows the secondary creep rate, elongation and creep rupture strength of every superalloy. In this table, secondary creep rate, elongation and rupture strength were respectively estimeted as secondary creep rate at the stress of 3.4 kg/mm$^2$, minimum elongation at the time to rupture of 1000hr and mean rupture strength at the time of 1000hr. It is easily recognized from this table that electron beam weld joint is rather comparable to base metal in both secondary creep rate and elongation than TIG weld joint. Meanwhile, there is no appreciable dif-

**Table 8** Evaluation of Creep and Creep Rupture Properties for Base Metal and Weld Joint

| Material and Specimen | | Secondary Creep Rate at 3.4kg/mm² (%/hr) | Minimum Value of Elongation at Fracture of 1000 hr (%) | Mean Rupture Strength at 1000hr (kg/mm²) |
|---|---|---|---|---|
| HAEN | Base Metal | — | 30 | 4.4 |
| | EB Weld Joint | — | 12 | 〃 |
| | TIG Weld Joint | — | 7 | 〃 |
| HAEM | Base Metal | $1 \times 10^{-2}$ | 20 | 3.6 |
| | EB Weld Joint | $7 \times 10^{-3}$ | 〃 | 〃 |
| | TIG Weld Joint | $5 \times 10^{-4}$ | 5 | 〃 |
| HVEN | Base Metal | — | 31 | 3.4 |
| | EB Weld Joint | — | 〃 | 〃 |
| | TIG Weld Joint | — | 10 | 2.4 |
| Inconel 625 | Base Metal | — | 35 | 2.6 |
| | EB Weld Joint | — | 〃 | 〃 |
| | TIG Weld Joint | — | 17 | 〃 |
| Inconel 617 | Base Metal | — | 41 | 5.0 |
| | EB Weld Joint | — | 18 | 〃 |
| | TIG Weld Joint | — | 〃 | 〃 |
| Incoloy 800 | Base Metal | — | 28 | 2.8 |
| | EB Weld Joint | — | 〃 | 〃 |
| | TIG Weld Joint | — | 1 | 2.3 |
| Incoloy 807 | Base Metal | — | 43 | 3.4 |
| | EB Weld Joint | — | 21 | 〃 |
| | TIG Weld Joint | | 〃 | 〃 |

Gauge Length : 30 mm

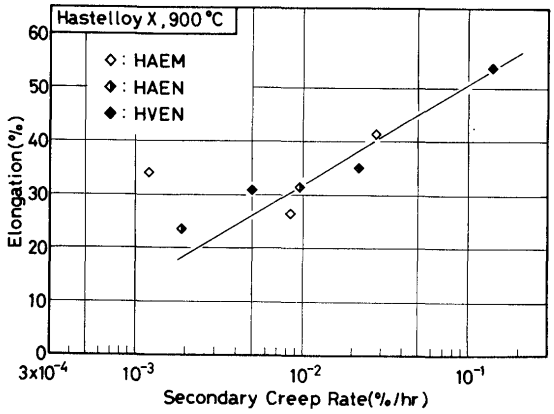


**Fig. 16** Relation between Secondary Creep Rate and Elongation

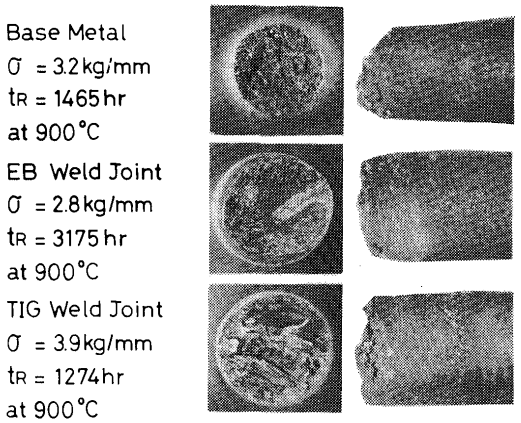


**Photo. 1** Macro-view of Fractured Specimen of Hastelloy X (HAEM)

ference between base metal and weld joint. Therefore, electron beam weld joint is considered to be rather resistant against the fracture in creep and creep rupture properties for above-mentioned reason than TIG weld joint, considering the fracture of welded pipe due to the creep deformation.

### 6.2.4 Obervation of Test Specimen after Fracture

#### (1) Appearance of Test Specimen

The characteristics of fracture morphology is common with every superalloy in the appearance. **Photo. 1** shows one of typical examples for HAEM base metal, its electron beam and TIG weld joint. In case of base metal, fracture surface is rather rugged. In case of electron beam weld joint, fracture takes place at considerably flat surface. In case of TIG weld joint, fracture takes place at rather rugged surface selectively along the dendritic boundary. Test specimen of base metal accompanies a few surface cracks adjacent to the fracture position. In the test specimen of weld joint, meanwhile, surface crack is hardly

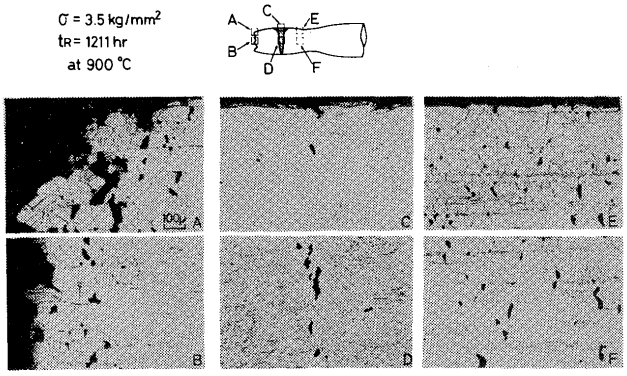


Photo. 2 Microstructure of Electron Beam Weld Joint Specimen of Hastelloy X (HAEM) Fractured at Base Metal

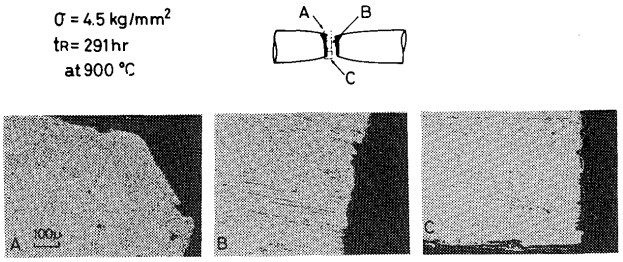


Photo. 3 Microstracture of Electron Beam Weld Joint Specimen of Hastelloy X (HAEM) Fractured at Weld Metal

observed.

## (2) Microstructure

The characteristics of microstructure adjacent to the fracture position was recognized in base metal, electron beam weld joint and TIG weld joint respectively irrespective of the material as mentioned below.

**Photo. 2** describes typical fracture mechanism for test specimen of base metal. As shown in this photo., many voids are observed at the grain boundary. From this characteristics, it is easily estimated that fracture has taken place through the connection of these voids. The rugged fracture surface shown in **Photo. 1** seems to have resulted from this fracture mechanism.

In case of electron beam weld joint, very few voids are observed at the boundary of columnar structure. However, many ones are observed at the interface in the middle area of the welds as shown in **Photo. 2.** These voids connect with each other, and main crack propagates rather straightly in case of fracture at weld metal zone as shown in **Photo. 3.** Considerably flat fracture surface of electron beam weld joint shown in **Photo. 1** results from this mechanism of crack propagation.

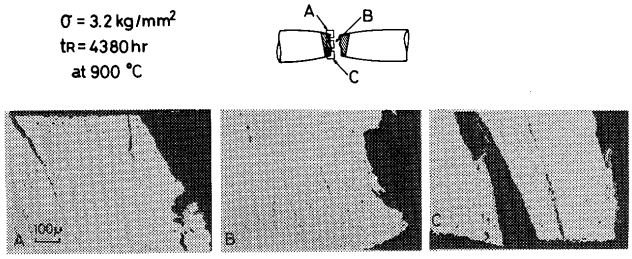


Photo. 4 Microstructure of TIG Weld Joint Specimen of Hastelloy X (HAEM) Fractured at Weld Metal

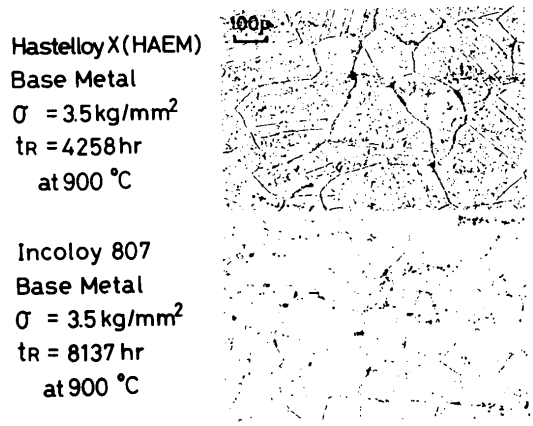


Photo. 5 Typical Change of Precipitate under Creep Rupture Test

fracture surface of electron beam weld joint shown in **Photo. 1** results from this mechanism of crack propagation.

In case of TIG weld joint fractured at the weld metal zone, cracks and voids occur at the surface of weld metal zone and at the boundary of columnar structure respectively. In TIG weld joint, the direction of formation of columnar structure and loading one make the angle of 45° approximately. Therefore, voids due to the slipping is easily made at the boundary of columnar structure. The crack at the surface connects with these voids with the elapse of time, and fracture seems to take place as shown in **Photo. 4.** The characteristics of fracture shown in **Photo. 1** results from this fracture mechanism.

In case of Ni-base superalloy, carbides precipitate both at the grain boundary and in the matrix without distinction of base metal and weld metal, and these carbides start to cohere with the elapse of time. Meanwhile, the quantity of carbides is rather small in case of Fe-base superalloy. **Photo. 5** shows typical example.

## 7. Conclusion

In this report, base metal of superalloys for nuclear plants, its electron beam and TIG weld joint were compared with each other in the mechanical properties. Obtaind conclusions are summarized as follows.

1) TIG weld joint is superior to electron beam weld joint and base metal in 0.2% proof stress irrespective of the material, and electron beam weld joint is also superior to base metal. There is appreciable difference of tensile stress between base metal and weld joint regardless of the materials. Meanwhile, electron beam weld joint is superior to TIG weld joint in both elongation and reduction of area.
weld joint in both elongation and reduction of area.
2) Electron beam weld joint has considereably higher low-cyle fatigue properties at elevated temperatures than TIG weld joint, and it is usually as high as base metal.
3) In the scondary creep rate, base metal of Hastelloy X (HAEM) has higher one than its weld joint. However, electron beam weld joint is nearly comparable to the base metal.
4) There is hardly any appreciable difference between base metal and weld joint in the creep rupture strength without distinction of the material. In the ductility, base metal is most superior and is followed by electron beam weld joint and TIG weld joint in the order of high ductility. However, electron beam weld joint is rather comparable to base metal.
5) In consideration of welded pipe with circumferential joint, weld joint should be evaluated in terms of secondary creep rate, elongation and rupture strength. As the weld joint of high creep rupture strength approaches the base metal in the secondaly creep rate and elongation, it seems to be more resistant against the fracture due to creep deformation. In this point of view, electron beam weld joint is far superior to TIG weld joint and nearly comparable to the base metal.

### References

1) Shuji TAIRA, "Thermal Stress and Thermal Fatigue (in Japanese)", The Industrial Daily News Ltd. (1974)
2) S. SHIMIZU, K. SATOH, M. KIYOSHIGE, H. MURASE and J. FUJIOKA, "Creep properties of Hastelloy X and their Application to the Structural Design (in Japanese)", Report Published by The 123rd Com. of Japan Society for the Promotion of Science, Vol. 16 (1975), No. 3, P319 ~P338.